Biofuels Production from Hydrothermal Decarboxylation of Oleic Acid and Soybean Oil Over Ni-based Transition Metal Carbides Supported on Al-SBA-15

Basem Al Alwan[a], Steven O. Salley[a,b], and K. Y. Simon Ng[a,b,c,*]

[a] *Department of Chemical Engineering and Materials Science, Wayne State University, Detroit, MI 48202, USA*

[b] *National Biofuels Energy Laboratory, NextEnergy, Detroit, MI 48202, USA*

[c] *Alternative Energy Technology, Wayne State University, Detroit, MI 48202, USA*

Abstract

Several Ni-based transition metal carbide catalysts supported on Al-SBA-15 were studied for the hydrothermal decarboxylation of oleic acid and soybean oil to produce diesel range hydrocarbons with no added H_2. The effect of pre-reduction, sub-critical and super-critical water conditions on the catalyst activity and selectivity was investigated. Both the conversion of oleic acid and selectivity of decarboxylation products under super-critical conditions for each catalyst were about 2-times greater than at sub-critical conditions. In addition, the potential of these catalysts for utilizing aqueous phase reforming (APR) of glycerol for *in situ* H_2 production to meet process demands was demonstrated. The performance of the catalysts increases with the addition of glycerol, especially for the NiWC/Al-SBA-15 catalyst. With the addition of glycerol, the NiWC/Al-SBA-15 catalyst showed greater conversion of oleic acid and selectivity to heptadecane; however, most of the oleic acid was hydrogenated to produce stearic acid. The highest conversion of oleic acid and selectivity for heptadecane was 97.3% and 5.2%, respectively. Furthermore, the NiWC/Al-SBA-15 catalyst exhibited good potential for hydrolyzing triglycerides (soybean oil) to produce fatty acids and glycerol, and then generating H_2 *in situ* from the APR of the glycerol produced. A complete conversion of soybean oil and hydrogenation of produced oleic acid were obtained over the NiWC/Al-SBA-15 at super-critical conditions.

---

[*] Corresponding author. Tel: 313-577-3805, Fax: 313-577-3810, Email address: sng@wayne.edu

Keywords:

Hydrothermal decarboxylation

Super-critical water

Oleic acid

Ni-based transition metal carbide catalysts

Generation of *in situ* H_2

1. Introduction

Biofuels production has been attracting considerable attention because of increases in petroleum prices and the world's energy demand, declines in petroleum reserves, and concerns about the environmental issues associated with greenhouse gas emissions. Triglycerides and fatty acids (from plants, animal fat, and waste oil/grease) can be used as renewable fuel feedstocks [1, 2]. Eliminating oxygen from triglycerides and fatty acids in the form of H_2O, CO, or CO_2 produces renewable liquid biofuels that are similar to petroleum fuels and can be directly used in existing infrastructure with no modifications [3, 4]. The cost of biofuels production from new vegetable oils is not likely to be competitive with the cost of petroleum fuels. Therefore, using inexpensive and inedible feedstocks such as waste oil and brown grease is necessary to produce biofuels that are fungible with petroleum fuels. The hydrocracking process is the most developed route for removal of oxygen from triglycerides and fatty acids to produce biofuels [5-7]. Our previous study [8] has shown that bimetallic carbide catalysts (NiWC/Al-SBA-15) prepared by a Dendrimer-Encapsulated-Nanoparticles (DENP) method with a Ni-W ratio of 2:1 led to a complete conversion of DDGS corn oil (>95% triglycerides) over 16 continuous days with 100% diesel selectivity for 4 days at 400 °C and 4.48 MPa. However, this process requires high pressure of H_2 and has issues related to catalyst deactivation due to the presence of water [9, 10].

An alternative method for removing oxygen is decarboxylation of fatty acid, a method which proceeds under lower H_2 pressure [11]. Most reports have focused on the use of noble metal catalysts, Pd [12-14] or Pt. [15-17] Also, some early studies focused on the decarboxylation of fatty acids in hydrocarbon solvents such as dodecane over Pd-supported catalysts [18-22]. Several studies showed that using water as solvent for the decarboxylation of fatty acids is more advantageous than hydrocarbon solvents [23-25], not only because water is an environmentally friendlier solvent but also the avoidance of a water removal step after triglycerides hydrolysis that generates fatty acids in an aqueous stream. Watanabe et al. [26] studied the effect of the addition of alkali hydroxide (NaOH and KOH) and metal oxides (CeO_2, Y_2O_3, and ZrO_2) on the decarboxylation of stearic acid in super-critical water at 400 °C. KOH promoted the monomolecular decarboxylation of stearic acid to produce C_{17} alkane and CO_2, while ZrO_2 was effective for bimolecular decarboxylation into C_{16} alkene and CO_2 because long chain ketone was observed. For the decarboxylation of palmitic acid in sub-critical water at 370 °C, 63% and 76% pentadecane molar yields were obtained over 5% Pd/C and 5% Pt/C, respectively [27]. Although the catalysts experienced a reduction in metal dispersion after the reaction, these changes did not seem to reduce their activities. However, the cost and rapid deactivation due to catalyst coking [19] and lack of H_2 [28], hindered the use of these catalysts commercially.

Fu et al. [29] reported that activated carbons could be an alternative to the expensive noble metal catalysts to convert saturated and unsaturated fatty acids to alkanes in sub and super-critical water. Although the major products were alkanes that are produced via decarboxylation and hydrogenation of oleic acid after 3 h at 370 °C, only 6% molar yield of decarboxylation product was obtained.

Triglycerides, a type of neutral lipids, can be rapidly hydrolyzed in hydrothermal media to produce saturated and unsaturated free fatty acids, as well as glycerol [30]. Some studies examined hydrothermal catalytic reforming of glycerol, commonly referred to as aqueous phase reforming (APR), to generate hydrogen [31-36]. Utilizing glycerol APR for *in situ* hydrogen production can promote the hydrogenation of unsaturated fatty acids. The addition of Re to Pt/C catalyst can motivate the glycerol APR due to the reduction of the affinity for CO [34, 37]. A complete conversion of oleic acid was achieved over Pt-Re/C catalyst when a 1:3 glycerol-to-oleic acid molar ratio was applied in a 2 h reaction. The catalyst experienced moderate sintering, suggesting additional work is needed to investigate its hydrothermal stability with time on stream. Vardon et al. [30] proposed an integrated catalytic hydrothermal reaction for the conversion of triglycerides to hydrocarbon fuels with *in situ* hydrogen production from glycerol. A continuous hydrogen supply can be obtained by the APR of glycerol released from triglyceride hydrolysis.

To the best of our knowledge, there has been no study of the hydrothermal decarboxylation of fatty acids over Ni-based transition metal carbide catalysts supported on Al-SBA-15. If sufficiently active, these catalysts could be suitable low cost catalysts for the hydrothermal decarboxylation of fatty acids. Also, unlike noble metal catalysts, these catalysts are not sensitive to CO that is produced during fatty acid decarbonylation [38]. In the present work, we investigate the use of Ni-based transition metal carbide catalysts on an Al-SBA-15 for the decarboxylation in sub and super-critical water of unsaturated fatty acid (oleic acid) and triglycerides (soybean oil) to produce hydrocarbons in the diesel range without adding hydrogen.

2. Experimental

2.1. Materials

Ammonium (*para*)tungstate hydrate ($H_{42}N_{10}O_{42}W_{12}$. xH_2O, 99.99%, Aldrich), ammonium niobate(V) oxalate hydrate ($C_4H_4NNbO_9$. xH_2O, 99.99%, Aldrich), ammonium molybdate ($H_{24}Mo_7N_6O_{24}$. $4H_2O$, Sigma-Aldrich), zirconium(IV) oxynitrate hydrate (N_2O_7Zr. xH_2O, 99%, Aldrich), and nickel(II) nitrate hexahydrate (N_2NiO_6. $6H_2O$, Sigma-Aldrich) were used as W, Nb, Mo, Zr, and Ni sources, respectively. Oleic acid (technical grade 90%), aluminum isopropoxide ($C_9H_{21}AlO_3$, 99.99%), heptane (UN1206, 99%), the mesoporous silica

SBA-15, glycerin (Class IIIB) were purchased from Sigma-Aldrich, Aldrich, EMD Chemicals, Advanced Chemicals Supplier (ACS), and Fisher-Scientific, respectively.

2.2. Catalyst preparation

A neutral support, SBA-15, with a 9 nm pore diameter and Brunauer-Emmett-Teller (BET) surface area of 600 m^2/g, was modified by aluminum isopropoxide to adjust its acidity. The advantages of using SBA-15 as a support in this study are its high surface-to-volume ratio, relatively wide pore size to minimize the resistance to triglycerides diffusion, and high thermal stability [39,40]. Moreover, lacking of Brønsted acidity allows modifying the acidity of pure siliceous SBA-15 to control the cracking activities [41]. SBA-15 (20 g) was suspended in hexane (150 mL); then, aluminum isopropoxide (0.067 g) was added to the solution and stirred for 24 h. The mixture was filtered, dried, and calcined at 550 °C for 4 h. According to our previous work [8], the catalysts NiNb, NiMo, NiW, and NiZr were prepared in the ratio of 6.67 wt% Ni:3.33 wt% M (M = Nb, Mo, W, Zr) by the wet co-impregnation of aqueous solutions of ($Ni(NO_3)_2$. $6H_2O$, $C_4H_4NNbO_9$. xH_2O), ($Ni(NO_3)_2$. $6H_2O$, $(NH_4)_6Mo_7O_{24}$. $4H_2$), ($Ni(NO_3)_2$. $6H_2O$, $(NH_4)_{10}(H_2W_{12}O_{42})\cdot 4H_2O$), and ($Ni(NO_3)_2$. $6H_2O$, $ZrO(NO_3)_2\cdot$ xH_2O) on the modified Al-SBA-15 support. The resulting solids were dried and calcined at 450 °C for 4 h.

Carburization was conducted using temperature-programmed reduction (TPR) according to the method of Claridge et al. [42]. Each metal oxide precursor was placed in a quartz tube and subjected to a flow of 20% CH_4/80% H_2 at 30 cm^3/min and a heating rate of 10 K/min to 250 °C, followed by 2.0 K/min to 730 °C. The temperature was maintained at 730 ^oC, the optimal temperature for carbide formation, for 30 min to complete the reaction [42]. After cooling, the catalyst was passivated under a mixture of 1% O_2 in Ar for 1 h to eliminate its pyrophoricity [43] and protect the bulk of the catalyst against deep oxidation [44].

2.3. Material characterization

X-Ray diffraction (XRD) patterns were collected using a Rigaku RU2000 rotating anode powder diffractometer (Rigaku Americas Corporation, TX) with SmartLab Guidance and MDI Jade 8 software at a scan rate of 8 °/min. Scanning Electron Microscopy (JSM-7600 FE SEM) equipped with Pegasus Apex 2 integrated EDS and EBSD Systems with capabilities of Spectral Imaging, OIM Data Collection and analysis with high accuracy and high efficiency was used to determine the composition of the catalysts.

2.4. Reaction procedure

The catalytic hydrothermal decarboxylation of oleic acid was conducted in unstirred mini-reactors assembled from 3/8-inch stainless steel Swagelok parts, sealed with a cap on each end to give a reactor volume of 1.52 mL [27]. The advantage of using 316L stainless steel reactors to carry out the reaction under sub- and super-critical water is the high contents of Cr and Ni [45]. The protective Cr_2O_3 layer on the steel surface prevents the metal leaching. The 316L stainless steel reactor shows good stability when it was exposed to supercritical water at 480 ^{o}C/25 MPa for 120 h. Prior to use in any experiments, the reactors were washed with acetone and water to remove any residual materials. In typical experiments, 10 mg catalyst, 0.642 mL water, and 0.156 mmol oleic acid were loaded in the reactors. The reactors were sealed in a glove box to avoid their exposure to air. The loaded reactors were placed in a pre-heated furnace (400 ^{o}C) and (350 ^{o}C) to achieve super-critical and sub-critical conditions, respectively. After the desired reaction time was completed (4 h), the reactors were submerged in a water bath to quench the reaction. The products were transferred to volumetric flasks, and the reactors were rinsed with repeated heptane washes until the total volume collected was 10 mL.

Additional experiments were performed with the same catalysts that were reduced in H_2 before being loaded to the reactors to investigate the effect of a catalyst reduction step. During the reduction, the catalysts were placed in a quartz tube reactor and reduced in H_2 (30 mL/min) at 450 ^{o}C for 3 h. After cooling to ambient temperature, the ends of the tube were quickly sealed and placed in a glove box to minimize the likelihood of re-oxidation of the reduced catalysts.

Another set of experiments was conducted by adding different loadings of glycerol to the reactants to determine the impact of glycerol as a hydrogen donor. Three different glycerol loading were applied (0.12, 0.24, and 0.48 mmol glycerol). The experiments were carried out under super-critical conditions.

Finally, soybean oil was used as a feedstock to investigate the ability of the catalysts to hydrolyze the triglycerides to form fatty acids and glycerol; and then produce hydrogen *in situ* from the generated glycerol. Therefore, no addition glycerol is required for the hydrothermal decarboxylation of triglycerides. These experiments were conducted under super-critical conditions.

2.5. Analysis method

The liquid products were analyzed using a Perkin Elmer Clarus 500 gas chromatograph (GC) equipped with flame ionization detector (FID) and an Rtx-65 TG column (Restek, 17008, length: 30 m, internal diameter: 0.25 mm, phase film thickness: 0.10 μm). For fatty acid separation, the GC oven temperature was programmed as follows: 1 min hold at 80 ^{o}C, 30 ^{o}C/min ramp to 240 ^{o}C, 0 min hold at 240 ^{o}C, 10 ^{o}C/min ramp to 360 ^{o}C, 15 min hold at 360 ^{o}C. The detector temperature was maintained at 360 ^{o}C. Samples (1.5 μL) were injected into the column with a 5:1 split ratio. For hydrocarbon analysis, the GC oven temperature was programmed as follows: 2 min hold at 40 ^{o}C, 10 ^{o}C/min ramp to 300 ^{o}C, 5 min hold at 300 ^{o}C. The injector and detector temperatures were 250 ^{o}C and 300 ^{o}C, respectively, and the split ratio was 5:1. Concentrations were determined by the external standard method.

In order to identify the products, a gas chromatography-mass spectrometer (GC-MS) (Clarus 500 GC-MS, Perkin-Elmer) with a capillary wax Rtx-WAX column (length: 60 m, diameter: 0.25 mm, thickness of stationary phase 0.25 μm) was also used.

3. Results and discussion

3.1. Catalyst characterization

The XRD patterns of the nickel-based carbide catalysts with four different metals (Mo, Nb, W, and Zr) supported on Al-SBA-15 are shown in Fig. 1. For all the catalysts, the broad peak between $2\theta = 15–30°$ corresponds to the mesoporous silica. The XRD patterns of the catalysts show three main peaks at $2\theta = 44.6^{o}$, 52.2^{o}, and 76.3^{o}, corresponding to the (111), (200), and (220) diffractions of the Ni particles, respectively [24]. There is no indication of Ni carbide formation, confirming that Ni metal was easily reduced to form Ni particles, in agreement with the findings of Gajbhiye et al. [26]. The carbide phases of Mo, Nb, and W were observed; however, the carbide phase of Zr was not observed, which may suggest that the Zr carbide phase was very well dispersed on the support or the particles were too small to be detected by XRD [29].

SEM incorporated with EDAX was used to determine the composition of the catalysts in terms of Ni, transition metals (Mo, Nb, W, Zr), Al, and Si content as shown in Fig. 2. The metal loading was approximately 10 wt% with Ni:M (M = Mo, Nb, W, Zr) ratio of 2:1 for each catalysts.

3.2. Effect of sub- and super-critical water on hydrothermal decarboxylation of oleic acid

Four different catalysts for the hydrothermal decarboxylation of oleic acid under sub-critical conditions (350 ^{o}C and 16.5 MPa) and super-critical conditions (400 ^{o}C and 32 MPa) were evaluated. As a control experiment, hydrothermal decarboxylation of oleic acid in super-critical water was conducted in the absence of catalyst with only 4.7% conversion observed, which is in agreement with Fu et al. [29] Also, the influence of the support (Al-SBA-15 with no metals) on the hydrothermal decarboxylation of oleic acid was studied under supercritical conditions and showed similar conversion to that observed for the control experiment.

Table 1 summarizes the results for the hydrothermal decarboxylation of oleic acid under super-critical conditions after 4 h reaction time for the four catalysts supported on Al-SBA-15. All of the catalysts exhibited similar conversion of oleic acid (30-33 %) which can be attributed to the absence of rich H_2 environment. The major product of the reaction from every catalyst was unsaturated C17 arising directly from decarboxylation and decarbonylation reactions. The NiWC/Al-SBA-15 produced heptadecane with a selectivity of 0.72%; while less than 0.1% heptadecane selectivity was obtained from the other catalysts. These results suggest that the NiWC/Al-SBA-15 has slightly higher activity for the hydrogenation reaction than others. This may be attributed to the variation in the valence shell for tungsten and the other metals (Mo, Nb, and Zr). The electrons in tungsten's valence shell (5d) have higher average energy than the electrons in the other metal's valence shell (4d). Therefore, the hydrogenation activity of tungsten catalyst was higher than the other metal catalysts. The GC-FID spectrum of the product obtained from the NiWC/Al-SBA-15 catalyst, Fig. 3, shows that an oxygenated compound (γ-Stearolactone) was observed in the product at a level of roughly 21-35% for all of the catalysts. The double bond in the oleic acid migrates from the position of (Δ9) to the (Δ4) position before ring closure resulted in the γ-Stearolactone [46]. The presence of the double bond in oleic acid may promote oligomerization paths that produce higher molecular weight materials, which do not elute from the GC-FID. Table 2 shows the identities and selectivites of the minor products for the hydrothermal decarboxylation of oleic acid after 4 h reaction in super-critical water. The products, unsaturated C11-C16, suggest that the catalysts possess some cracking activity. Although Fu et al. [29] shows that the conversion of oleic acid over activated carbon after 3 h at 370 ^{o}C was 80%, the selectivity of heptadecane was only 7%. Also, only partial hydrogenation of oleic acid (31%) to stearic acid took place over Pt/C after 9 h at 300 ^{o}C [27, 30].

A proposed mechanism of hydrothermal decarboxylation of oleic acid in super-critical water based on the previous results is shown in Fig. 4. During the hydrothermal decarboxylation of oleic acid, the carboxylic acid donates protons by the heterolytic cleavage of the O-H bond, generating a carboxylate and hydrogen ions. Heptadecenes (unsaturated C17) are produced due to the removal of CO_2. The *in situ* generated hydrogen (as a result of heterolytic cleavage of the O-H bond in oleic acid) is consumed by the hydrogenation of oleic acid or unsaturated C17 to form stearic acid or heptadecane, respectively. The produced stearic acid is then decarboxylated to generate more heptadecane. Moreover, hydrogen molecules can also be generated from water-gas shift reactions [47]. A similar sequential hydrogenation–decarboxylation pathway for oleic acid in dodecane solvent was proposed by Immer et al. [48]

The catalysts were evaluated for the hydrothermal decarboxylation activities of oleic acid in sub-critical water (350 ^{o}C) (Table 3). Under sub-critical conditions, all of the catalysts exhibited lower conversion and product selectivity for the hydrothermal decarboxylation of oleic acid than for super-critical conditions. The major products were oxygenated compounds, with no measurable amount of stearic acid. These results suggest that higher temperature promotes the hydrogenation-decarboxylation reactions of oleic acid. The decarboxylation of oleic acid over Pt/SAPO-11 after 2 h increased from 20% to 90% as the temperature increased from 200 °C to 325 °C. Also, the heptadecane selectivity increased by a factor of 4 when the temperature increased to 325 °C [49]. At super-critical conditions, water becomes a highly reactive medium due to the reduction in dielectric constant and increasing in self-dissociation constant [30].

The pretreatment (pre-reduction) of the catalysts did not significantly affect the hydrothermal decarboxylation of oleic acid at super-critical conditions (400 °C) for 4 h reaction (Fig. 5), which indicates that the pre-reduction step was not necessary because there was not much oxide on the catalyst surface. A similar finding by Fu et al. [27] shows that the pre-reduction step of Pt/C and Pd/C catalysts did not alter the catalyst activity for the hydrothermal decarboxylation of palmitic acid. Also, the pre-reduction of activated carbon did not show a significant effect on the hydrothermal decarboxylation of palmitic acid [29].

3.3. Effect of adding glycerol on hydrothermal decarboxylation of oleic acid

The effect of *in situ* H_2 production via glycerol APR (eq. 1) on the hydrothermal decarboxylation of oleic acid in super-critical water was examined. The need for external hydrogen is a basic challenge for conventional lipid hydrotreatment processes [11, 50]; however, the production of *in situ* hydrogen may alleviate this challenge.

$$C_3H_8O_3 + 3\,H_2O \longrightarrow 7\,H_2 + 3\,CO_2 \qquad \text{(eq. 1)}$$

Three different initial glycerol loadings were investigated for the hydrothermal decarboxylation of oleic acid at super-critical condition as shown in Fig. 6. Theoretically, the 0.156 mmol of oleic acid requires 0.156 mmol of H_2 to completely hydrogenate the oleic acid into stearic acid as shown in (eq. 2).

$$C_{18}H_{34}O_2 + H_2 \longrightarrow C_{18}H_{36}O_2 \qquad \text{(eq. 2)}$$

Based on eq. 1, the three initial glycerol loadings (0.12 mmol, 0.24 mmol, and 0.48 mmol) can generate H_2 of 0.84 mmol, 1.68 mmol, and 3.36 mmol, respectively. The NiMoC, NiNbC, and NiZrC supported on Al-SBA-15 performed similarly with the three different glycerol loadings as shown in Fig. 6. A slight increase in the stearic acid selectivity (Fig. 6 b) and decrease in the unsaturated C17 selectivity (Fig. 6 d) were observed when 0.12 mmol of glycerol was added. Also, the NiMoC, NiNbC, and NiZrC catalysts required higher glycerol loading (0.48 mmol) in order to obtain higher oleic acid conversion (Fig. 6 a). However, a significant improvement in the conversion of oleic acid (Fig. 6 a), selectivity of stearic acid (Fig. 6 b), and selectivity of heptadecane (Fig. 6 c) was observed for the reaction over NiWC catalyst with the addition of only 0.12 mmol of glycerol. The conversion of oleic acid and selectivity of heptadecane over NiWC catalyst reached 97.3% and 5.2% after adding 0.48 mmol glycerol. However, the production of unsaturated C17 decreased with the addition of glycerol (Fig. 6 d), which suggests that the direct decarboxylation of oleic acid decreased. These results suggest that hydrogenation of oleic acid dominates the reaction in the presence of excess H_2 to produce stearic acid. A complete hydrogenation of oleic acid into stearic acid and partial decarboxylation of stearic acid to produce heptadecane (24%) was observed when the reaction was carried out over Pt/C at 300 ^{o}C for 9 h, suggesting that the hydrogen concentration greatly affects the catalyst decarboxylation performance [30].

The addition of glycerol to the reactants of the hydrothermal decarboxylation of oleic acid improved the conversion of oleic acid and the selectivity of heptadecane. Fig. 6 illustrates a comparison of the catalyst performance before and after adding glycerol, indicating that all the catalysts utilized the glycerol for generating hydrogen. However, the NiWC/Al-SBA-15 exhibited the greatest potential for utilizing the *in situ* produced H_2 from glycerol to hydrogenate the oleic acid and then decarboxylate the produced stearic acid to produce heptadecane. The higher hydrogenation activity of the NiWC/Al-SBA-15 catalyst in comparison to others may be attributed to its fractional sum of electronegativity that falls in the range of electronegativity of noble metal catalysts [51]. Therefore, the rates of adsorption and desorption are similar to those observed for the noble metals. In addition, the high electron energy in the outermost shell of tungsten may be another reason for the higher activity of NiWC/Al-SBA-15 in comparison to the other catalysts.

A reaction sequence as shown in Fig. 7 is likely wherein the hydrogenation of oleic acid initially takes place to produce stearic acid followed by decarboxylation of stearic acid to form heptadecane. A similar finding by Vardon et al. [30] suggested that the hydrogenation of oleic acid to produce stearic acid, and followed by decarboxylation of the stearic acid over (Pt/C and Pt-Re/C) increased after adding glycerol. Although Pt/C and Pt-Re/C showed higher production of heptadecane than the catalysts in this study, the CO produced during fatty acid decarbonylation can inhibit the activity of those noble catalysts [38].

The product distributions obtained from the NiWC/Al-SBA-15 catalyst were influenced by the glycerol addition (0.48 mmol) as shown in Fig. 8. The oxygenated products that were produced from the hydrothermal decarboxylation of oleic acid with no glycerol addition diminished after adding the glycerol. Also, some shorter hydrocarbons (C10-C16) were apparent in the GC-FID spectrum, suggesting that the NiWC/Al-SBA-15 catalyst exhibited some cracking activity.

3.4. Conversion of lipids (soybean oil) to hydrocarbons

The process that is used to hydrolyze triglycerides to produce free fatty acids and glycerol in hydrothermal media is commonly called “fat-splitting” [46, 52, 53]. The previous experimental results support the idea of using triglyceride-based biomass such as soybean oil as a feedstock to produce hydrocarbons via hydrothermal decarboxylation reaction. No additional glycerol is required since glycerol molecules are generated from the hydrolysis of triglycerides. Following hydrolysis, liberated glycerol can undergo catalytic APR reactions to generate H_2 [30]. Also, glycerol can be catalytically decomposed to generate CO that is consumed to produce additional H_2 from the water-gas shift reaction.

A nearly complete conversion of soybean oil (>95% triglycerides) was obtained from the hydrothermal decarboxylation reaction to produce heptadecane, unsaturated C17, unsaturated C18, stearic acid, oleic acid, and linoleic acid as shown in Table 4. The soybean oil used in this study had a fatty acid profile of 2-5% stearic acid, 20-30% oleic acid, 50-60% linoleic acid and 5-11% linolenic acid. All of the catalysts exhibited good hydrolysis activities of triglycerides. The soybean oil (triglycerides) is converted to its major fatty acids (oleic acid and linoleic acid) in addition to other fatty acids such as stearic acid and linolenic acid. Also, the presence of stearic acid suggests that some of the oleic acid and linoleic acid were hydrogenated to produce stearic acid. Although several studies show that the rate of hydrogenation of linoleic acid is greater than oleic acid [54-56], the selectivity for hydrogenation of linoleic acid decreases as temperature increases [57]. A 19-31% selectivity to unsaturated C17 was observed for each catalyst, indicating a decarboxylation of oleic acid and linoleic acid took place. No oleic acid was observed when the reaction was carried out over the NiWC/Al-SBA-15. Also, the highest stearic acid selectivity was obtained from the NiWC/Al-SBA-15; therefore, this catalyst has the best hydrogenation activity, as observed previously. The results for the NiWC/Al-SBA-15 suggest that heptadecane was produced from either the decarboxylation of stearic acid or from the hydrogenation of unsaturated C17.

4. Conclusion

Catalytic hydrothermal decarboxylation processing is a promising method for converting low-quality lipid feedstocks, such as brown grease, which are typically high in free fatty acids and triglycerides, into hydrocarbon fuels. Several catalysts, Ni-based transition metal carbides supported on Al-SBA-15, were investigated for the hydrothermal decarboxylation of oleic acid. The effect of catalyst reduction, sub- and super-critical conditions on the catalysts performance was examined. Super-critical water promotes the hydrogenation-decarboxylation reactions of oleic acid due to the increase of water reactivity at super-critical temperature. Water at super-critical condition becomes a more reactive medium with lower dielectric constant and higher self-dissociation constant. The utilization of APR of glycerol for *in situ* hydrogen production motivates the hydrogenation of oleic acid to stearic acid and production of heptadecane especially over NiWC-Al-SBA-15. The NiWC/Al-SBA-15 showed higher hydrogenation activity than other catalysts, which may be attributed to its fractional sum of electronegativity that falls in the range of electronegativity of noble metal catalysts and the high electron energy in the outermost shell of tungsten. The NiWC/Al-SBA-15 shows a great potential to hydrolyze triglycerides, generate *in situ* H_2 from glycerol, hydrogenate oleic acid and linoleic acid to form stearic acid, and produce heptadecane. However, further hydrothermal decarboxylation of stearic acid is needed to enhance the selectivity to green diesel hydrocarbons. It is envisioned a bifunctional catalyst, or a two-step process can be developed for hydrothermal decarboxylation of triglycerides: first step for hydrogenation of unsaturated fatty acids over a modified NiWC/Al-SBA-15, and second step for decarboxylation of saturated fatty acid to produce alkanes. Thus, modified NiWC/Al-SBA-15 catalysts may provide an economically viable process for the hydrothermal decarboxylation of fatty acids and triglycerides derived from low-quality sources without the need of additional H_2.

Acknowledgements

Financial support from the Department of Energy (Grant DEFG36-05GO85005) and the National Institute of Food and Agriculture (Grant MICW-2010-01534) for this research are gratefully acknowledged.

References

[1] F. Ma, M. A. Hanna, Bioresour. Technol. 70 (1999) 1–15.

[2] X. Meng, J. Yang, X. Xu, L. Zhang, Q. Nie, M. Xian, Renewable Energy 34 (2009) 1–5.

[3] R. Sotelo-Boyás, Y. Liu, T. Minowa, Ind. Eng. Chem. Res. 50 (2010) 2791–2799.

[4] J. Gusmão, D. Brodzki, G. Djéga-Mariadassou, R. Frety, Catal. Today 5 (1989) 533–544.

[5] http://www.nesteoil.com/default.asp?path = 141, 11,991, 12,243, 15,658. 12,335.

[6] http://www.uop.com/processing-solutions/biofuels/green-diesel/#green- diesel biodiesel.

[7] http://www.dynamicfuelsllc.com/compare.aspx.

[8] B. Al Alwan, E. Sari, S. Salley, K. Y. S. Ng, Ind. Eng. Chem. Res. 53 (2014) 6923-6933.

[9] B. Peng, X. Yuan, C. Zhao, J. A. Lercher, J. Am. Chem. Soc. 134 (2012) 9400–9405.

[10] E. Laurent, B. Delmon, J. Catal. 146 (1994) 281–291.

[11] E. Santillan-Jimenez, M. Crocker, J. Chem. Technol. Biotechnol. 87 (2012) 1041–1050.

[12] I. Kubicková, M. Snåre, K. Eränen, P. Mäki-Arvela, D. Y. Murzin, Catal. Today 106 (2005) 197–200.

[13] M. Snåre, I. Kubicková, P. Mäki-Arvela, K. Eränen, J. Wärnå, D.Y. Murzin, Chem. Eng. J. 134 (2007) 29–34.

[14] P. Mäki-Arvela, M. Snåre, K. Eränen, J. Myllyoja, D.Y. Murzin, Fuel 87 (2008) 3543–3549.

[15] P. T. Do, M. Chiappero, L. L. Lobban, D. E. Resasco, Catal. Lett. 130 (2009) 9–18.

[16] M. Chiappero, P. T. M. Do, S. Crossley, L. L. Lobban, D. E. Resasco, Fuel 90 (2011) 1155–1165.

[17] J. G. Na, B. E. Yi, J. K. Han, Y. K. Oh, J. H. Park, T. S. Jung, S. S. Han, H. C. Yoon, J. N. Kim, H. Lee, C. H. Ko, Energy 47 (2012) 25–30.

[18] M. Snare, I. Kubickova, P. Maki-Arvela, D. Chichova, K. Eranen, D. Y. Murzin, Fuel 87 (2008) 933-945.

[19] M. Snare, I. Kubickova, P. Maki-Arvela, K. Eranen, D. Y. Murzin, Ind. Eng. Chem. Res. 45 (2006) 5708-5715.

[20] S. Lestari, P. Maki-Arvela, K. Eranen, J. Beltramini, G. Q. M. Lu, Murzin, D. Y, Catal Lett 134 (2010) 250-257.

[21] I. Simakova, O. Simakova, P. Maki-Arvela, A. Simakov, M. Estrada, D. Y. Murzin, Applied Catalysis A: General 355 (2009) 100-108.

[22] W. L. Roberts, H. H. Lamb, L. F. Stikeleather, T. L. Turner, US 7,816,570 B2, 2010.

[23] G. W. Huber, J. A. Dumesic, Catalysis Today 111 (2006) 119–132.

[24] D. Kusdiana, S. Saka, Appl. Biochem. Biotechnol. 115 (2004) 781–91.

[25] L. Li, E. Coppola, J. Rine, J. L. Miller, D. Walker, Energy Fuels 24 (2010) 1305–1315.

[26] M. Watanabe, T. Iida, H. Inomata, Energy Conversion and Management 47 (2006) 3344–3350.

[27] J. Fu, X. Lu, P. E. Savage, Energy Environ. Sci. 3 (2010) 311–317.

[28] H. Bernas, K. Eranen, I. Simakova, A. R. Leino, K. Kordas, J. Myllyoja, P. Maki-Arvela, T. Salmi, D. Y. Murzin, Fuel 89 (2010) 2033–2039.

[29] J. Fu, F. Shi, L. T. Thompson, X. Lu, P. E. Savage, ACS Catal. 1 (2011) 227–231.

[30] R. Vardon, B. Sharma, H. Jaramillo, D. Kim, J. Choe, P. Ciesielski, T. Strathmann, Green Chem. 16 (2014) 1507-1520.

[31] R. D. Cortright, R. R. Davda, J. A. Dumesic, Nature 418 (2002) 964–967.

[32] J. Shabaker, G. Huber, J. Dumesic, J. Catal. 222 (2004) 180–191.

[33] N. Luo, X. Fu, F. Cao, T. Xiao, P. P. Edwards, Fuel 87 (2008) 3483–3489.

[34] D. L. King, L. Zhang, G. Xia, A. M. Karim, D. J. Heldebrant, X. Wang, T. Peterson, Y. Wang, Appl. Catal. B 99 (2010) 206–213.

[35] D. Ö. Özgür, B. Z. Uysal, Biomass Bioenergy 35 (2011) 822–826.

[36] L. Zhang, A. M. Karim, M. H. Engelhard, Z. Wei, D. L. King, Y. Wang, J. Catal. 287 (2012) 37–43.

[37] E. L. Kunkes, D. A. Simonetti, J. A. Dumesic, W. D. Pyrz, L. E. Murillo, J. G. Chen, D. J. Buttrey, J. Catal. 260 (2008) 164–177.

[38] R. R. Soares, D. A. Simonetti, J. A. Dumesic, Angew. Chem., Int. Ed. 118 (2006) 4086–4089.

[39] W. Stevens, K. Lebeau, M. Mertens, G. van Tendeloo, P. Cool, E. Vansant, J. Phys. Chem. B 110 (2006) 9183–9187.

[40] F. Zhang, Y. Yan, H. Yang, Y. Meng, C. Yu, B. Tu, D. Zhao, J. Phys. Chem. 109 (2005) 8723–8732.

[41] H. Wang, S. Yan, S. Salley, S. Ng, Fuel 111 (2013) 81–87.

[42] J. B. Claridge, A. P. E. York, A. J. Brungs, Chem. Mater. 12 (2000) 132–142.

[43] W. Zhang, Y. Zhang, L. Zhao, W. Wei, Energy Fuels 24 (2010) 2052–2059.

[44] L. Leclercq, A. Almazouari, M. Dufour, G. Leclercq, in The Chemistry of Transition Metal Carbides and Nitrides, S. T. Oyama, ed., Springer, Netherlands (1996) 345–361.

[45] X. Luo, R. Tang, C. Long, Z. Miao, Q. Peng, C. Li, Nuclear Eng. & Tech. 40 (2007) 147–154.

[46] S. C. Cermak, T. A. Isbell, JAOCS 77 (2000) 243-248.

[47] R. L. Holliday, J. W. King, G. R. List, Ind. Eng. Chem. Res. 36 (1997) 932–935.

[48] J. G. Immer, M. J. Kelly, H. H. Lamb, Applied Catalysis A: General 375 (2010) 134-139.

[49] M. Ahmadi, E. E. Macias, J. B. Jasinski, P. Ratnasamy, M. A. Carreon, J. of Molec. Catal. A: Chemical 386 (2014) 14-19.

[50] A. Berenblyum, V. Danyushevsky, E. Katsman, T. Podoplelova, V. Flid, Pet. Chem. 50 (2010) 305–311.

[51] B. Al Alwan, S. Salley, K.Y.S. Ng, Applied Catalysis A: General 485 (2014) 58–66.

[52] L. Lascaray, Ind. Eng. Chem. 41 (1949) 786–790.

[53] T. A. Patil, D. N. Butala, T. S. Raghunathan, H. S. Shankar, Ind. Eng. Chem. Res. 27 (1988) 727–735.

[54] A. J. Dijkstra, J. of the American Oil Chemists' Society 77 (2000) 1329-1331.

[55] A. Šmidovnik, I. Plazl, T. Koloini, Chemical Engineering Journal 51 (1993) B51-B56.

[56] M. B. Fernández, G. M. Tonetto, G. Crapiste, D. E. Damiani, Journal of Food Engineering 82 (2007) 199-208.

[57] G. Díaz, R. Perez, N. Tapanes, D. Aranda, A. Arceo, Natural Science 3 (2011) 530-534.

List of Table Captions:

Table 1. Conversion and product selectivity for the hydrothermal decarboxylation of oleic acid after 4 h reaction in super-critical water.

Table 2. Identities and selectivities of minor products for the hydrothermal decarboxylation of oleic acid after 4 h reaction in super-critical water.

Table 3. Conversion and product selectivity for the hydrothermal decarboxylation of oleic acid after 4 h reaction in sub-critical water.

Table 4. Product selectivity for the hydrothermal decarboxylation of soybean oil after 4 h reaction in super-critical water.

Table 1

Catalyst on (Al-SBA-15)	Conversion (%)	Selectivity (%)				Liquid product wt. (%)
		C17	C17*	C18	C18*	
NiMoC	32.8	0.08	62.5	0	3.1	87
NiNbC	30.7	0	67.6	0	1.9	89
NiWC	30.7	0.72	53.6	0.04	1.8	91
NiZrC	30.1	0.09	67.7	0	1.1	86

* Unsaturated components

Table 2

Product	Selectivity (%)			
	NiMoC	NiNbC	NiWC	NiZrC
C11*	1.8	1.2	1.0	1.7
C12*	1.6	0.7	0.5	1.5
C13*	1.7	1.1	1.2	0.9
C14*	1.2	1.2	0.9	1.0
C15*	1.8	1.2	1.6	0.9
C16*	1.1	0.9	2.7	1.4
Stearic acid	1.6	1.4	1.9	1.3
γ-Stearolactone	21.8	21.3	32.7	21.1

* Unsaturated components

Table 3

Catalyst on (Al-SBA-15)	Conversion (%)	Selectivity (%)				Liquid product wt. (%)
		C17	C17*	C18	C18*	
NiMoC	13.1	0	34.6	0	0.96	98
NiNbC	15.3	0	31.1	0	0.83	99
NiWC	15.6	0.01	35.8	0.03	1.01	97
NiZrC	12.9	0	28.5	0	0.77	97

* Unsaturated components

Table 4

Catalyst	Selectivity (%)						
	C17	C17*	C18	C18*	Stearic acid	Oleic acid	Linoleic acid
NiMoC	0.04	31.1	0	2.9	19.3	9.6	20.1
NiNbC	0.04	31.1	0	2.9	16.2	14.4	19.7
NiWC	2.1	19.7	0	3.7	39.6	0	15
NiZrC	0.03	30.5	0	2.6	14.3	18.2	21

* Unsaturated components

List of Figure Captions:

Fig. 1. XRD patterns of NiMoC/Al-SBA-15, NiWC/Al-SBA-15, NiZrC/Al-SBA-15, and NiNbC/Al-SBA-15.

Fig. 2. SEM and EDAX analysis of: NiMoC/Al-SBA-15 (a), NiNbC/Al-SBA-15 (b), NiWC/Al-SBA-15 (c), and NiZrC/Al-SBA-15 (d).

Fig. 3. GC-FID spectrum of the product obtained from the hydrothermal decarboxylation of oleic acid after 4 h reaction in super-critical water over the NiWC/Al-SBA-15 catalyst.

Fig. 4. Proposed reaction mechanism for the hydrothermal decarboxylation of oleic acid in super-critical water.

Fig. 5. Effect of the catalyst pre-reduction on the hydrothermal decarboxylation of oleic acid after 4 h reaction in super-critical water. Conversion of oleic acid and selectivity of unsaturated C17 (a), Selectivity of C17, C18, and unsaturated C18 (b).

Fig. 6. Conversion and product selectivity for the hydrothermal decarboxylation of oleic acid with different initial glycerol loading after 4 h reaction in super-critical water. Conversion of oleic acid (a), selectivity of stearic acid (b), selectivity of C17 (c), and selectivity of unsaturated C17 (d).

Fig. 7. Reaction sequence for the hydrothermal decarboxylation of oleic acid in the presence of glycerol in super-critical water.

Fig. 8. GC-FID spectrum of the product obtained from the hydrothermal decarboxylation of oleic acid with glycerol addition (0.48 mmol) after 4 h reaction in super-critical water over the NiWC/Al-SBA-15 catalyst.

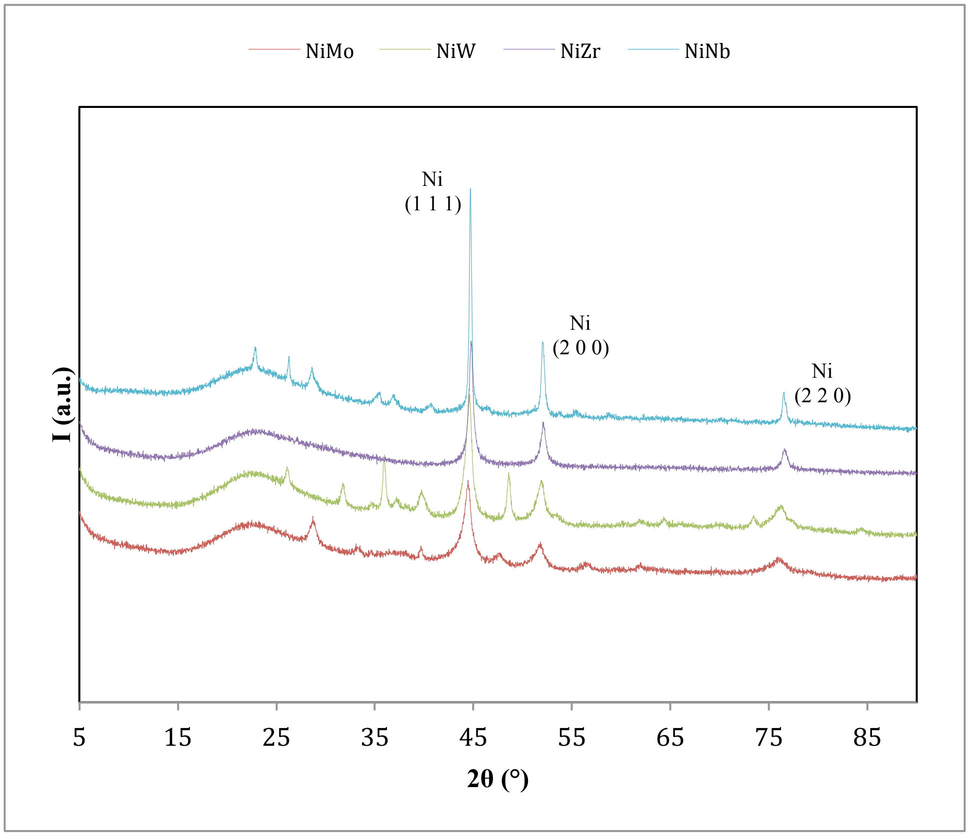
NiMo
NiW
NiZr
NiNb
Ni
(1 1 1)
Ni
(2 0 0)
Ni
(2 2 0)
I (a.u.)
5
15
25
35
45
55
65
75
85
2θ (°)

Fig. 1

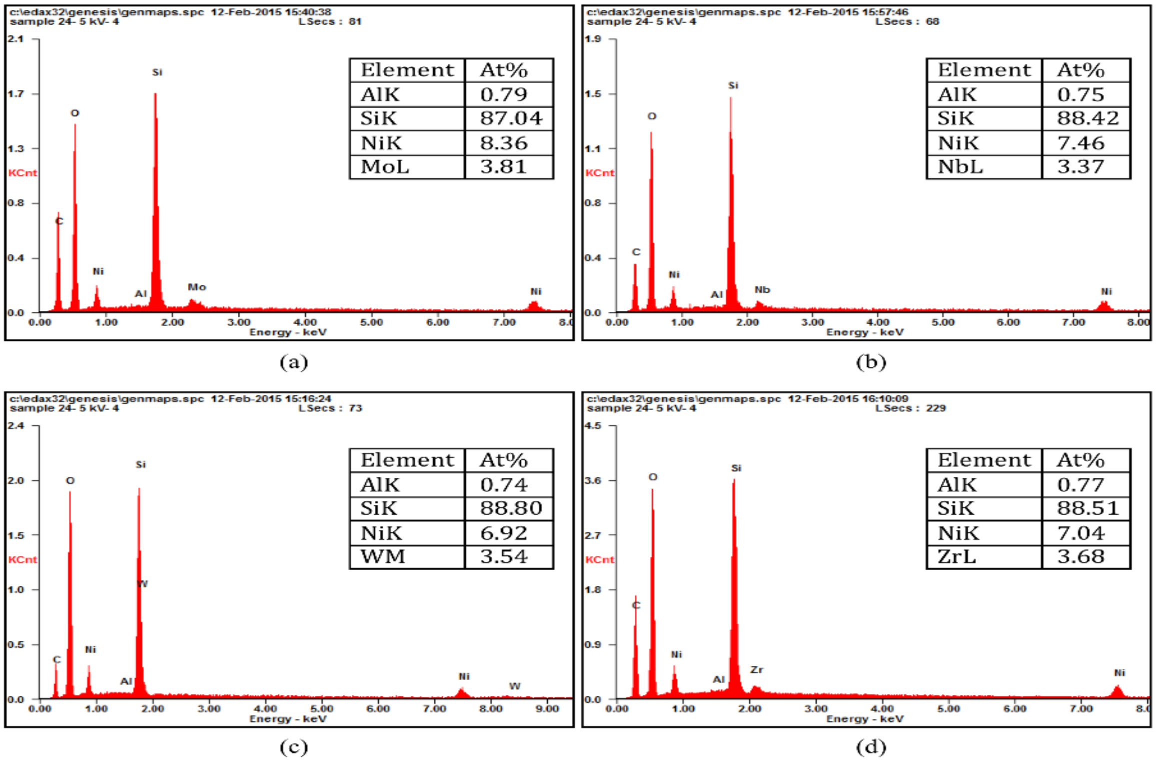

Element	At%
AlK	0.79
SiK	87.04
NiK	8.36
MoL	3.81

(a)

Element	At%
AlK	0.75
SiK	88.42
NiK	7.46
NbL	3.37

(b)

Element	At%
AlK	0.74
SiK	88.80
NiK	6.92
WM	3.54

(c)

Element	At%
AlK	0.77
SiK	88.51
NiK	7.04
ZrL	3.68

(d)

Fig. 2

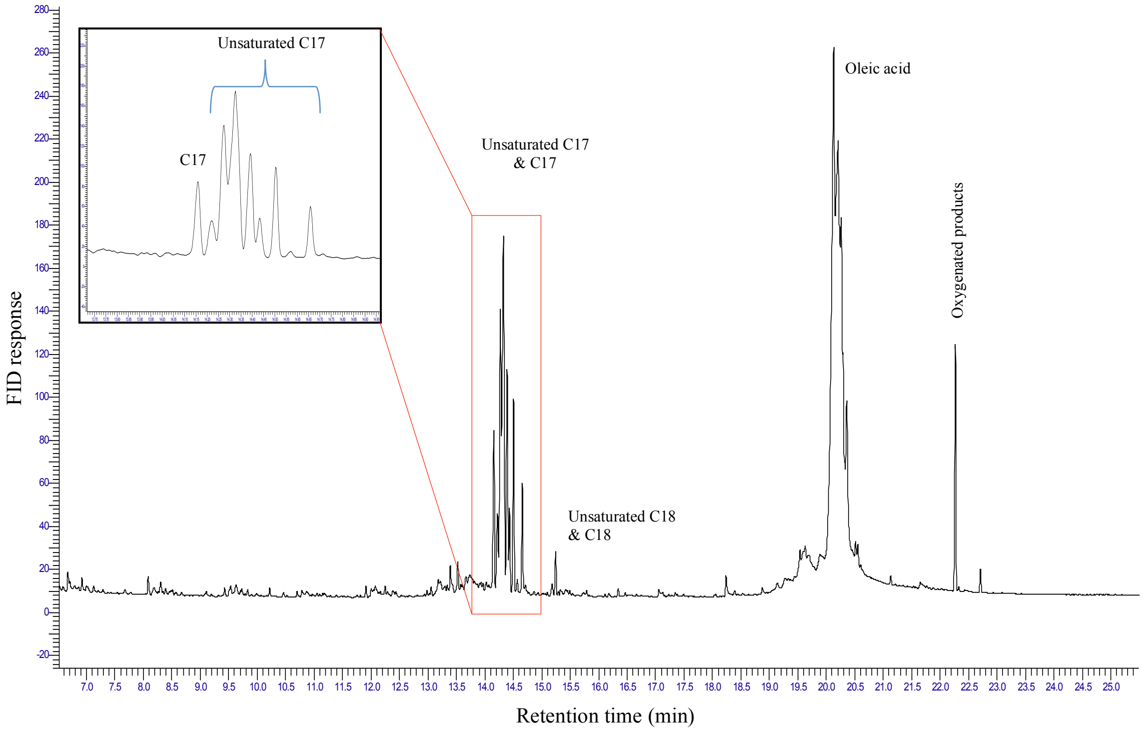
Unsaturated C17
C17
Unsaturated C17
& C17
Unsaturated C18
& C18
Oleic acid
Oxygenated products
FID response
280
260
240
220
200
180
160
140
120
100
80
60
40
20
0
-20
7.0
7.5
8.0
8.5
9.0
9.5
10.0
10.5
11.0
11.5
12.0
12.5
13.0
13.5
14.0
14.5
15.0
15.5
16.0
16.5
17.0
17.5
18.0
18.5
19.0
19.5
20.0
20.5
21.0
21.5
22.0
22.5
23.0
23.5
24.0
24.5
25.0
Retention time (min)

Fig. 3

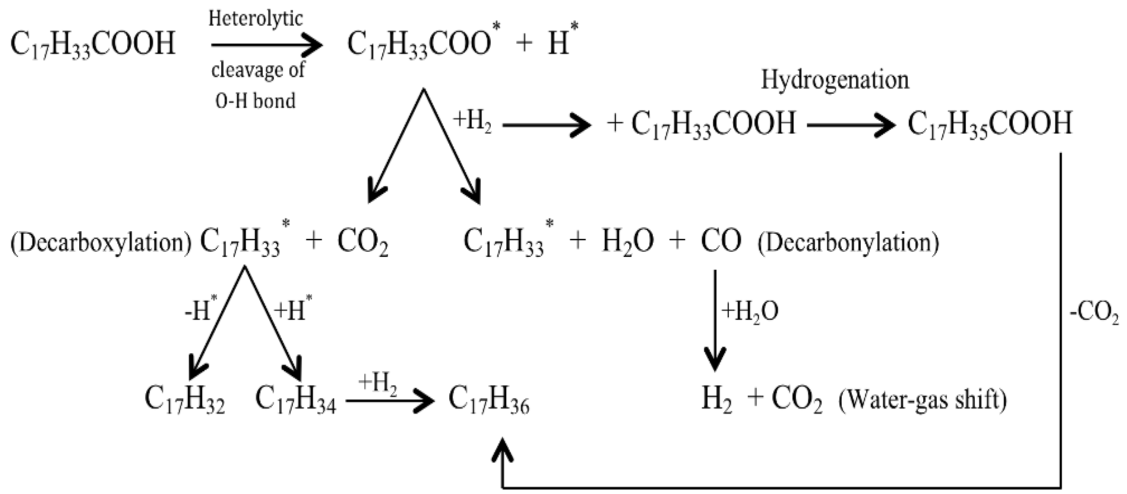
$C_{17}H_{33}COOH$
Heterolytic cleavage of O-H bond
$C_{17}H_{33}COO^* + H^*$
$+H_2$
Hydrogenation
$+ C_{17}H_{33}COOH$
$C_{17}H_{35}COOH$
(Decarboxylation) $C_{17}H_{33}^* + CO_2$
$C_{17}H_{33}^* + H_2O + CO$ (Decarbonylation)
$-H^*$
$+H^*$
$+H_2O$
$-CO_2$
$C_{17}H_{32}$
$C_{17}H_{34}$
$+H_2$
$C_{17}H_{36}$
$H_2 + CO_2$ (Water-gas shift)

Fig. 4

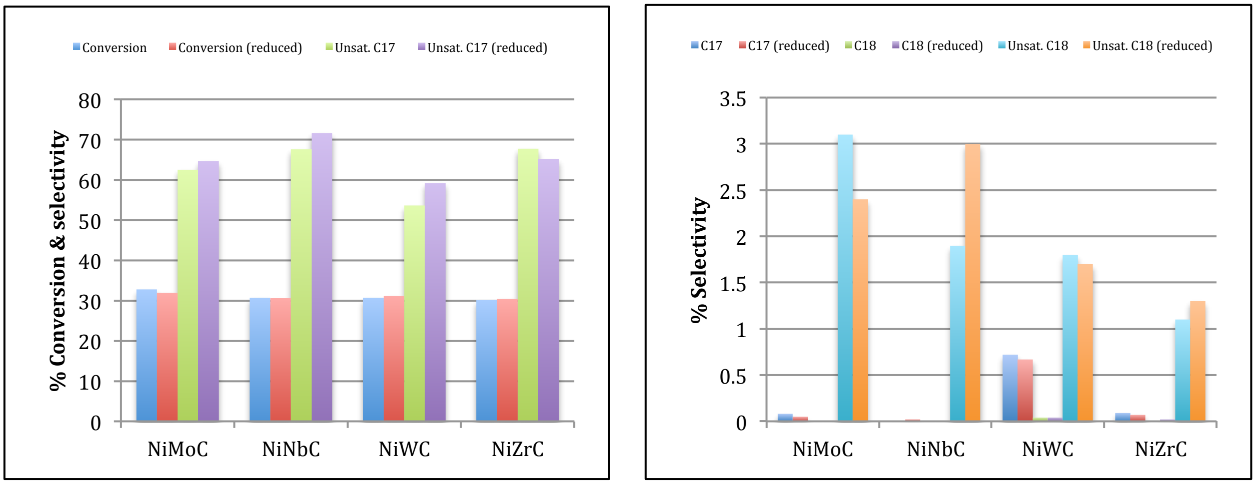
Conversion
Conversion (reduced)
Unsat. C17
Unsat. C17 (reduced)
% Conversion & selectivity
80
70
60
50
40
30
20
10
0
NiMoC
NiNbC
NiWC
NiZrC
C17
C17 (reduced)
C18
C18 (reduced)
Unsat. C18
Unsat. C18 (reduced)
% Selectivity
3.5
3
2.5
2
1.5
1
0.5
0
NiMoC
NiNbC
NiWC
NiZrC

(a) (b)

Fig. 5

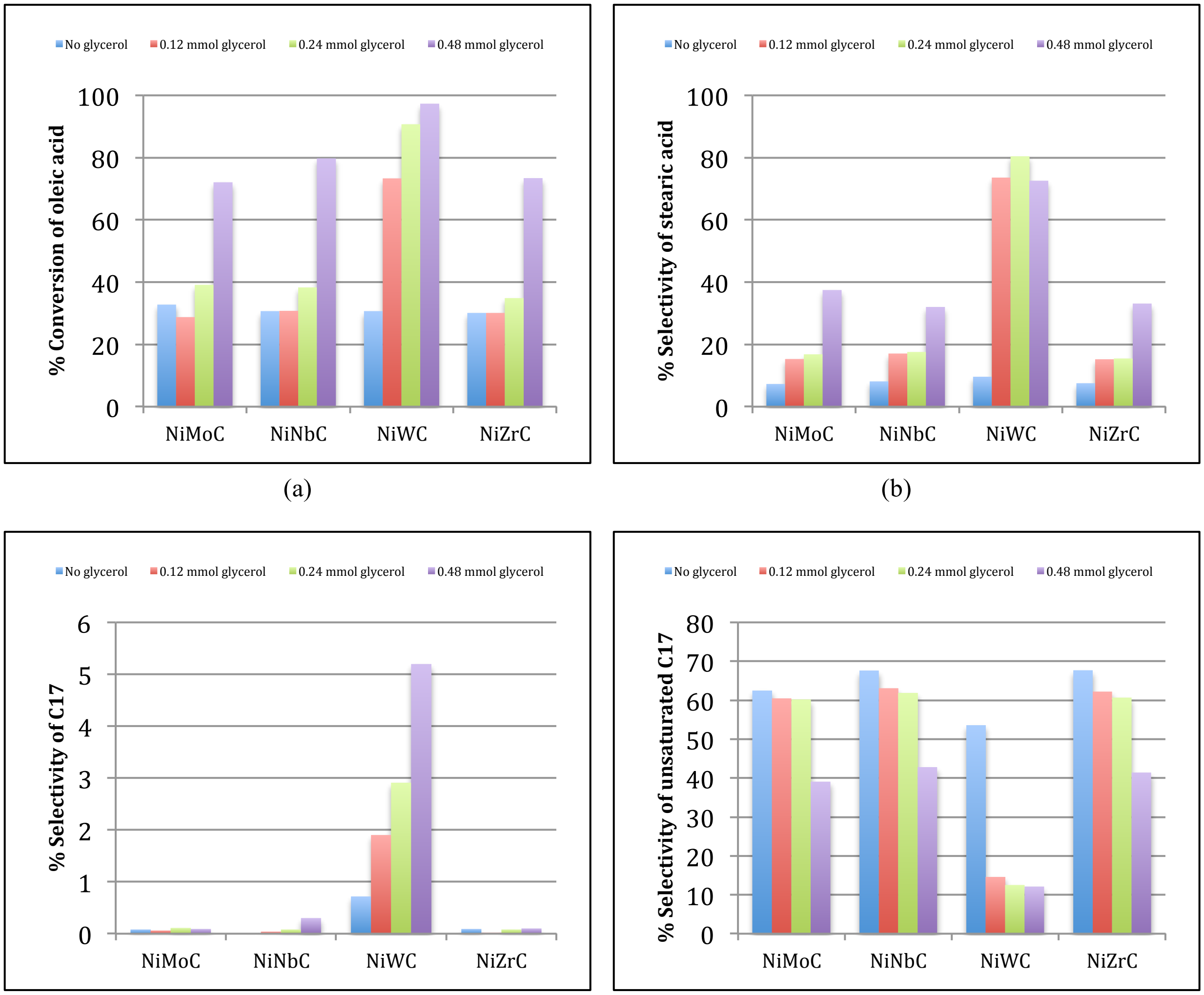
No glycerol
0.12 mmol glycerol
0.24 mmol glycerol
0.48 mmol glycerol
% Conversion of oleic acid
0
20
40
60
80
100
NiMoC
NiNbC
NiWC
NiZrC
% Selectivity of stearic acid
% Selectivity of C17
0
1
2
3
4
5
6
% Selectivity of unsaturated C17
0
10
20
30
40
50
60
70
80

(a) (b) (c) (d)

Fig. 6

$$C_3H_8O_3 + 3\,H_2O \longrightarrow 7\,H_2 + 3\,CO_2$$

$$C_{17}H_{33}COOH + H_2 \longrightarrow C_{17}H_{35}COOH$$

$$C_{17}H_{35}COOH \longrightarrow C_{17}H_{36} + CO_2$$

Fig. 7

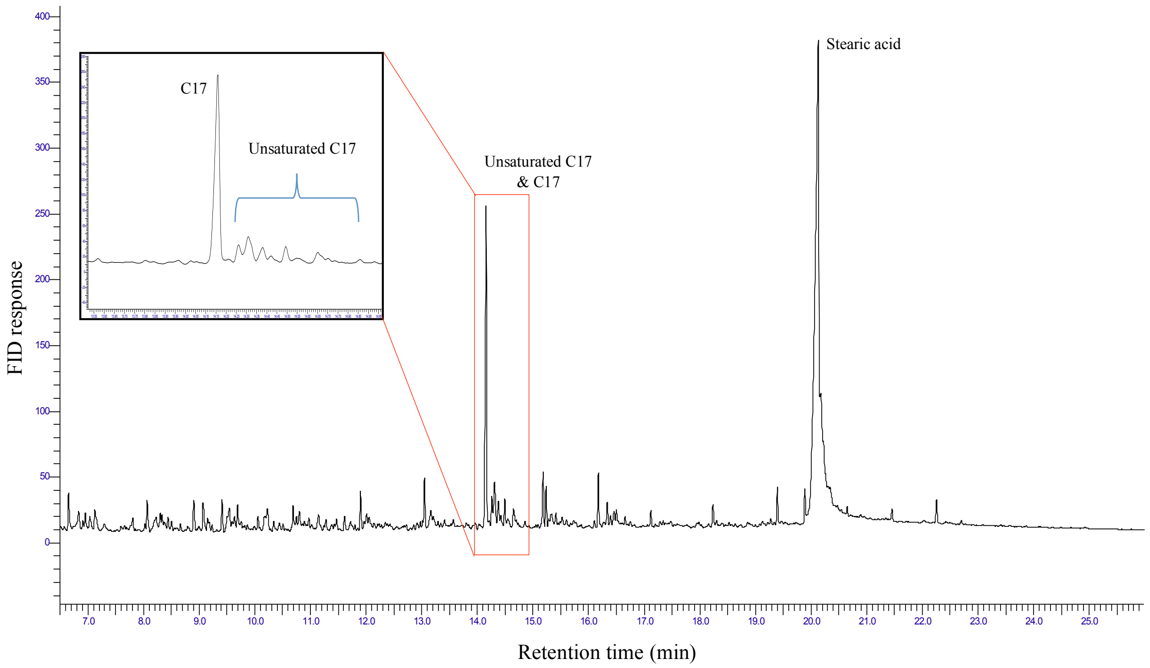
FID response
400
350
300
250
200
150
100
50
0
C17
Unsaturated C17
Unsaturated C17
& C17
Stearic acid
7.0
8.0
9.0
10.0
11.0
12.0
13.0
14.0
15.0
16.0
17.0
18.0
19.0
20.0
21.0
22.0
23.0
24.0
25.0
Retention time (min)

Fig. 8